ISTITUTO NAZIONALE DI RICERCA METROLOGICA
Repository Istituzionale

Quantification of the Void Volume in Single-Crystal Silicon

(Article begins on next page)

30 October 2024

Quantification of the Void Volume in Single-Crystal Silicon

Giancarlo D'Agostino[1]*, Marco Di Luzio[1-2], Giovanni Mana[1], Luca Martino[1], Massimo Oddone[2], and Carlo Paolo Sasso[1]

1 Istituto Nazionale di Ricerca Metrologica (INRIM), Strada delle Cacce 91, 10135 Torino, Italy

2 Department of Chemistry, University of Pavia, via Taramelli 12, 27100 Pavia, Italy

ABSTRACT: This paper investigates the use of a method based on Cu decoration and neutron activation to determine the total volume of voids in a silicon single crystal. A measurement protocol was developed and tested in an experiment carried out with a 5 cm^3 volume and 10 g mass high-purity natural silicon sample. The few percent uncertainty reached in the determination of the Cu concentration, at a 10^{14} cm^{-3} level, makes this method a candidate to set an upper limit to the concentration of the vacancies contributing to the void volume in the enriched silicon material used to determine the Avogadro constant.

The latest and most accurate value of the Avogadro constant, $N_A = 6.02214076(12) \times 10^{23}$ mol^{-1}, was obtained by counting the atoms of two 1 kg ^{28}Si-enriched spheres.[1] This result was achieved after refined measurements of the mass and volume of the spheres, and the atomic weight and lattice parameter of the ^{28}Si material used.

The N_A uncertainty depends mostly on the surface characterization and volume determination of the spheres. The presence of contaminants was extensively investigated using infrared spectrometry and neutron activation analysis and corrected for or demonstrated negligible.[2,3]

The crystal used was grown in vacancy mode; the vacancy concentration, $N_{vac} = 3.3(1.1) \times 10^{14}$ cm^{-3}, was measured by positron lifetime spectroscopy.[4,5] Typical grown-in defects are voids formed by vacancy aggregation; cavities bigger than 50 nm in diameter were excluded by laser scanning topography.

Since positron annihilation detected only mono-vacancies, di-vacancies and similar small agglomerates, a method for determining the volume of voids smaller than 50 nm in diameter is highly valuable.

Quantification of the Void Volume. Spaepen suggested to determine the upper limit of the total volume of voids by filling them with silicide precipitates after Cu diffusion. Specifically, he proposed to diffuse Cu ions, provided by a copper-nitrate surface layer, into a single-crystal silicon sample by annealing it until the equilibrium concentration is reached.[6] The supersaturation of Cu in the subsequent slow cooling (1 °C min^{-1}) causes the Cu$_3$Si precipitation into voids of any size, mono-vacancies included.[7-9] The remaining interstitial Cu is out-diffused to the crystal surface by annealing at a lower temperature and eliminated by surface etching. Finally, the volume of voids is determined from the quantification of the Cu concentration and the knowledge of the Cu$_3$Si structure. Since defects other than voids might be precipitation sites for Cu silicide, the void volume is likely to be overestimated; therefore, it is accepted as an upper limit.

Spaepen proved that, when the sample is coated with a metallic Cu capping layer to limit the Cu out-diffusion to the surface during cooling, artificial voids in a Si wafer are completely filled with the η' phase of Cu$_3$Si. In addition, he showed that the Cu precipitates are stable if the subsequent out-diffusion time and temperature are kept limited.[10]

To quantify the final Cu concentration, Spaepen proposed to dissolve the sample, with the embedded Cu$_3$Si precipitates, and to measure the Cu amount by mass spectrometry.[10] As regards the Avogadro ^{28}Si material, based on the vacancy concentration obtained with the positron lifetime spectroscopy, the expected Cu concentration after the in- and out-diffusion is about 1.5×10^{15} cm^{-3}. Therefore, the quantification limit of the chemical analysis should be (at least) of the same order of magnitude.

As an alternative to mass spectrometry, we investigated the use of Instrumental Neutron Activation Analysis (INAA), because it avoids the sample dissolution and makes it possible to monitor the out-diffusion. In the following, we describe a measurement protocol developed and tested with a sample of high-purity natural single-crystal silicon. The sample was supersaturated to fill the voids with Cu$_3$Si. Subsequently, we measured the Cu concentration before and after successive out-diffusions, carried out to progressively remove the interstitial Cu. Under the assumption that the interstitial Cu out-diffuses completely, the Cu concentration is expected to stabilize to a lower value corresponding to the precipitated Cu. Eventually, based on the observed value, we estimated an upper limit to the concentration of the vacancies trapped into voids.

EXPERIMENTAL SECTION

Diffusion of Copper in Silicon. Cu has the highest solubility, among the transition metals, in Si; the equilibrium solubility, $S_{Cu}(T)$, as well the diffusivity coefficient, $D_{Cu}(T)$, strongly depends on temperature, T.[11-15] Therefore, annealing at high temperature and quenching to room temperature originate oversaturation; most of the interstitial Cu precipitates in the bulk or out-diffuses to the surface.[16] A slow cooling rate of about 1 °C min^{-1} is suggested to ensure diffusion of Cu without homogeneous precipitation.[10,16] At temperatures of about 400 °C, the equilibrium concentration of interstitial Cu drops to negligible levels, but Cu remains highly mobile. Therefore, annealing at this temperature promotes the out-diffusion of Cu to the surface.

We in-diffused Cu ions in the bulk of the Si sample by annealing at 740 °C to reach an equilibrium solubility of Cu in Si, S_{Cu}(740 °C), sufficient to decorate all the voids.

In order to grossly design the process, we solved the one dimensional diffusion equation to compute the concentration of Cu, N_{Cu}, as a function of time. In this model, an initially pure 10 mm thick Si slab of infinite extent is coated with a pure Cu layer and annealed at 740 °C. It is assumed that the Cu in-diffuses with a constant diffusivity coefficient, D_{Cu}(740 °C), from a substrate layer whose N_{Cu} is indefinitely kept at S_{Cu}(740 °C) = 2.2 × 10^{16} cm^{-3}.[13]

The in-diffusion time required to reach at the slab center 90 % of S_{Cu}(740 °C) varies from 5000 s to 6700 s, depending on the most recent D_{Cu}(740 °C) values we found in literature, i.e. 5.2 × 10^{-5} cm^2 s^{-1} and 3.8 × 10^{-5} cm^2 s^{-1}, respectively.[14,15]

We out-diffused Cu ions to the surface of the Si sample by annealing at 450 °C to reach a solubility value low enough to extract almost completely the interstitial Cu in a reasonable time.

The diffusion equation was solved again, now for a 10 mm Si (voids free) slab of infinite extent homogenously filled with interstitial Cu at a concentration $N_{Cu} = S_{Cu}$(740 °C). It is assumed that the Cu out-diffuses with a constant D_{Cu}(450 °C) to a surface layer whose Cu concentration is set indefinitely to $N_{Cu} = S_{Cu}$(450 °C) = 2.4 × 10^{13} cm^{-3}.[13]

The out-diffusion time required to reach S_{Cu}(450 °C) at the slab center the 450 °C S_{Cu} (in particular, 1 % above it), depending on the adopted D_{Cu}(450 °C) value, is reported in the first row of Table 1

Table 1. Calculated out-diffusion time, t_{out}, to reach S_{Cu}(450 °C) at the centre of a 10 mm Si slab initially filled with interstitial Cu at a concentration N_{Cu} (0 h); the result depends on the adopted diffusivity coefficient, D_{Cu}(450 °C).

N_{Cu} (0 h)	t_{out}	
	D_{Cu} = 8.6 × 10^{-6} cm^2 s^{-1} [14]	D_{Cu} = 1.7 × 10^{-5} cm^2 s^{-1} [15]
22 × 10^{15} cm^{-3}	26 h	14 h
1.3 × 10^{15} cm^{-3}	17 h	9 h

Preparation of the sample. The 10.5 g sample used in this study is a 5 cm length and 1 cm thick rectangular parallelepiped cut from a high-purity natural Si single crystal. The sample surface was cleaned by repeated cycles of (i) Cu deposition by galvanic displacement with a water solution of copper(II) nitrate, $Cu(NO_3)_2$ ($\rho_{Cu(NO3)2}$ = 60 g L^{-1}), and ammonium fluoride, NH_4F (ρ_{NH4F} = 30 g L^{-1}),[17] and subsequent (ii) removal by etching with a water solution of iron(III) chloride, $FeCl_3$, (ρ_{FeCl3} = 300 g L^{-1}). When the Cu deposition, about 0.5 μm thick, looked regular and without visible defects, it was left as the Cu source and capping layer.

The coated sample was annealed in vacuum at 740 °C using an electrical oven. The temperature was slowly increased starting from room temperature; the transient between 700 °C and 740 °C took about 3 h. At 740 °C, the oven was switched off and the sample left in it to ensure the Cu_3Si precipitation into the voids without formation of dislocation loops and stacking faults due to fast cooling;[10] the cooling rate reached a maximum of 3 °C min^{-1}, immediately after the oven was switched off, and gradually decreased to 1 °C min^{-1} in 10 h. Finally, the external Cu layer was removed by etching it with a 10:1 solution of nitric

acid, HNO$_3$, and hydrofluoric acid, HF, for 40 min. The mass removed by etching, 485 mg, corresponds to a surface Si layer about 100 μm thick. Figure 1 shows a picture of the sample after etching.
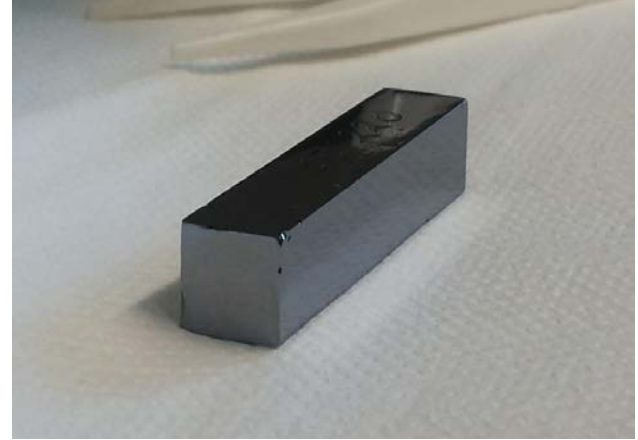

Figure 1. The Si sample after the deep etching following the annealing at 740 °C and slow cooling.

In order to monitor the out-diffusion, the residual interstitial Cu was removed step by step by a sequence of five out-diffusion cycles performed in air at 450 °C and annealing time limited to 2 h; the cooling rate was always less than 3 °C min^{-1}. The Cu drained to the surface was eliminated by etching the sample with HNO$_3$ – HF (10:1) for 3 min. The surface Si layer removed after each out-diffusion cycle was about 15 μm thick. The possible extra Cu precipitations, occurring between the surface and a depth of a few micrometers,[10] were eliminated.

Measurement of the Copper Concentration. The Cu concentrations after the in-diffusion at 750 °C and each out-diffusion at 450 °C were measured by INAA. The measurement was carried out by counting the 1345.8 keV γ-photons emitted in the decay of the ^{64}Cu produced by the activation of ^{63}Cu via the neutron capture reaction ^{63}Cu(n,γ)^{64}Cu.

The major radionuclides produced by ^{28}Si, ^{29}Si and ^{30}Si via neutron capture reactions are ^{28}Al, ^{29}Al and ^{31}Si. Since the half-lives of ^{28}Al and ^{29}Al are a few minutes, their γ-emissions disappear in a few hours whereas the γ-emission of ^{31}Si, whose half-life is 2.6 h, persists longer.

When the analysis concerns a single element, e.g. Cu, the relative standardization method is usually adopted. However, the detection of the ^{31}Si γ-emission from the sample makes itself a mono-elemental standard for the application of the k_0 standardization method based on an internal monitor.

In the case of the relative method, the Si sample, smp, is co-irradiated with a Cu standard, std, and the Cu concentration is given by

$$N_{Cu} = \frac{C_{\gamma 64_{Cu}}^{smp}}{C_{\gamma 64_{Cu}}^{std}} \frac{m^{std}}{m^{smp}} \frac{r_{63_{Cu}}^{std}}{r_{63_{Cu}}^{smp}} \frac{\varepsilon_{p,\gamma 64_{Cu}}^{std}}{\varepsilon_{p,\gamma 64_{Cu}}^{smp}} \frac{\rho_{Si} N_A}{M_{Cu}},$$ (1)

where m is the mass, $C_{\gamma 64_{Cu}}$ is the count rate of the 1345.8 keV ^{64}Cu γ-emission, $\gamma_{64_{Cu}}$, $r_{63_{Cu}}$ is the total to thermal (n,γ) activation rate ratio of ^{63}Cu, $\varepsilon_{p,\gamma 64_{Cu}}$ is the full-energy γ-peak detection efficiency of $\gamma_{64_{Cu}}$, and ρ_{Si} and M_{Cu} are the Si density

and Cu molar mass. For ease of notation, here and hereafter superscripts smp and std are occasionally omitted.

In the case of the k_0 method, the ^{30}Si of the sample acts as the monitor nuclide and the Cu concentration is given by

$$N_{Cu} = \frac{C_{\gamma_{64\,Cu}}^{smp}}{C_{\gamma_{31\,Si}}^{smp}} \frac{S_{31\,Si}}{S_{64\,Cu}} \frac{k_{0,Au}(^{30}Si, \gamma_{31\,Si})}{k_{0,Au}(^{63}Cu, \gamma_{64\,Cu})} \frac{r_{30\,Si}^{smp}}{r_{63\,Cu}^{smp}} \frac{\varepsilon_{p,\gamma_{31\,Si}}^{smp}}{\varepsilon_{p,\gamma_{64\,Cu}}^{smp}} \frac{\rho_{Si}\, N_A}{M_{Cu}} \quad (2)$$

where $C_{\gamma_{31\,Si}}$ is the count rate of the 1266.2 keV ^{31}Si γ-emission, $\gamma_{31\,Si}$, $r_{30\,Si}$ is the total to thermal (n,γ) activation rate ratio of ^{30}Si, $\varepsilon_{p,\gamma_{31\,Si}}$ is the full-energy γ-peak detection efficiency of $\gamma_{31\,Si}$, $k_{0,Au}(^{30}Si, \gamma_{31\,Si})$ and $k_{0,Au}(^{63}Cu, \gamma_{64\,Cu})$ are the k_0 factors of the Au comparator versus the monitor ^{30}Si for the $\gamma_{31\,Si}$ emission and versus the target ^{63}Cu for the $\gamma_{64\,Cu}$ emission, respectively, and $S_{31\,Si}$ and $S_{64\,Cu}$ are the saturation factors of ^{31}Si and ^{64}Cu, respectively.

Explicitly, in eqs 1 and 2, $r_{63\,Cu}$ and $r_{30\,Si}$ are given as

$$r = 1 + \frac{G_{ep}}{G_{th}} \frac{Q_0}{f}, \quad (3)$$

where G_{th} and G_{ep} are the thermal and epithermal neutron self shielding factors, respectively, Q_0 is the resonance integral to 2200 ms^{-1} neutron cross section ratio of the target nuclide for a $1/E$ epithermal neutron flux and f is the thermal to epithermal neutron flux ratio. In addition, $C_{\gamma_{64\,Cu}}$ and $C_{\gamma_{31\,Si}}$ are

$$C_\gamma = \frac{N_{p,\gamma}}{(t_c - t_{dead})} \frac{1}{D\,C}, \quad (4)$$

where $N_{p,\gamma}$ is the number of counts in the full-energy γ-peak, t_c is the counting time, t_{dead} is the dead time of the detection system, and $D = e^{-\lambda t_d}$ and $C = (1 - e^{-\lambda t_c})/\lambda t_c$ are the decay and counting factors (t_d is the decay time and $\lambda = \ln(2)/t_{1/2}$ is the decay constant of the produced radionuclide, given its half-life $t_{1/2}$). Lastly, $S = 1 - e^{-\lambda t_{irr}}$, where t_{irr} is the irradiation time.

Neutron Activation. The neutron activation lasted 6 h and was performed in the central channel of the 250 kW TRIGA Mark II reactor at the Laboratory of Applied Nuclear Energy (LENA) of the University of Pavia; the thermal and epithermal neutron fluxes were 6×10^{12} cm^{-2} s^{-1} and 5.5×10^{11} cm^{-2} s^{-1}, respectively.

A 3.6 mg Cu wire, 47 mm long, (Sigma-Aldrich, 0.1 mm diameter, 99.999% assay) was used as a standard. After weighing, it was sealed in a polyethylene microtube. As shown in Figure 2, the Si sample was closed in a polyethylene vial and placed, with the Cu standard, in the polyethylene container used for irradiation.
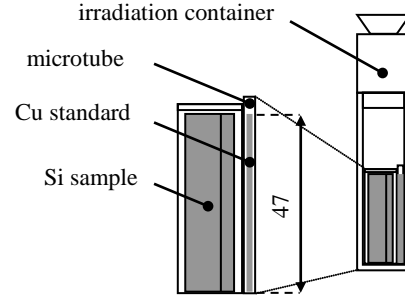

Figure 2. Si sample and Cu standard in the irradiation container. Dimension is in mm.

Gamma Spectrometry. After each neutron irradiation, the Si sample was removed from its vial, etched (HNO$_3$ – HF 10:1) for about 3 min to remove a possible external Cu contamination during handling and weighted. Two γ-spectra were sequentially recorded with a high purity germanium (HPGe) detector, ORTEC GEMS8530P4 (85 mm crystal diameter, 50 % crystal efficiency, 1.90 keV FWHM resolution at 1332 keV) connected to a ORTEC DSPEC jr 2.0 digital spectrometer for data acquisition. The first, smp$_1$, started 35 h after the irradiation and lasted 2.6 h with a relative dead time lower than 10 %. The second, smp$_2$, started 40 h after the irradiation and lasted 12.7 h with a relative dead time lower than 1 %.

As regards the Cu standard, four γ-spectra were sequentially collected without removing the polyethylene microtube to preserve the geometry. The first, std$_1$, started 150 h after the irradiation and lasted 5.5 h. The second, std$_2$, third, std$_3$, and fourth, std$_4$, were consecutively collected with the same acquisition time. The relative dead time was smaller than 10 %.

The positions of the Si sample and Cu standard during the γ-spectrometry measurements are shown in Figures 3a and 3b, respectively.
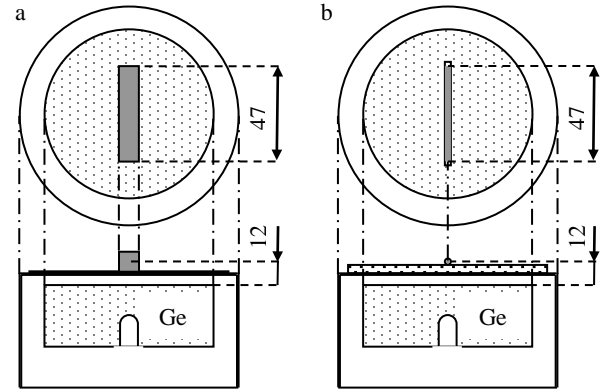

Figure 3. (a) Position of the Si sample and (b) of the Cu standard with respect to the Ge detector. Dimensions are in mm.

Gamma Peak Fitting. The $N_{p,\gamma_{64\,Cu}}$ and $N_{p,\gamma_{31\,Si}}$ values used to compute the count rates according to eq 4 were obtained by fitting the 1345.8 keV and 1266.2 keV peaks, respectively. The $C_{\gamma_{64\,Cu}}^{std}$ was determined from the std$_1$, std$_2$, std$_3$ and std$_4$ spectra, the $C_{\gamma_{64\,Cu}}^{smp}$ from the smp$_2$ spectrum and the $C_{\gamma_{31\,Si}}^{smp}$ from the smp$_1$ spectrum.

The curve fitting was performed with the ROI32 analysis engine of the Gamma Vision software.[18] Six channels were used for

background calculation within the region of interest of the peak for all the cases but for the ^{64}Cu peak of the sample, for which two channels were used. This choice allowed to limit the interference of the 1342.2 keV ^{28}Mg peak ($t_{1/2}$ = 20.9 h) produced by ^{29}Si via the threshold reaction ^{29}Si(n,2p)^{28}Mg to the 1345.8 keV ^{64}Cu peak shown in Figure 4.
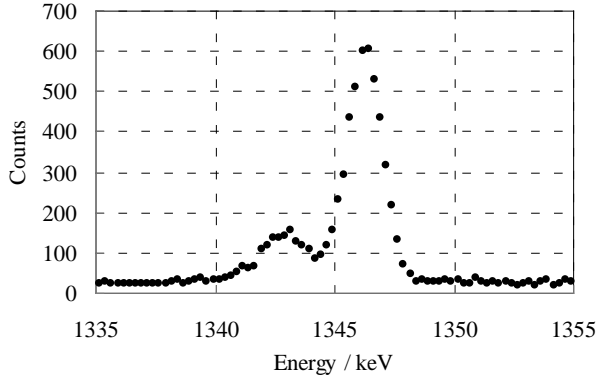

Figure 4. Zoom of a smp$_2$ γ-spectrum showing the 1345.8 keV ^{64}Cu peak and the interference of the 1342.2 keV ^{28}Mg peak.

Uncertainty Evaluation. The main advantage of the k_0 method is the possibility of using an internal monitor and, as a consequence, to avoid the position and geometry effects during the γ-counting. This is particularly important when the sample is located very close to the detector, as in this study. However, in the case of a ^{28}Si material there is only a trace amount of the ^{30}Si internal monitor and the application of the k_0 method is challenging.

As examples, the uncertainty budgets of the Cu concentration values measured after the fourth out-diffusion using the relative and k_0 method are shown in Tables 2 and 3, respectively. The uncertainty was evaluated according to the Guide to the Expression of Uncertainty in Measurement;[19]

Table 2. Uncertainty budget of the Cu concentration: relative method.

Quantity	Unit	Value	Standard uncertainty	Index
X	[X]	x_i	$u(x_i)$	%
$C^{smp}_{\gamma\,64\,Cu}$	s^{-1}	1.283	0.038	1.9
$C^{std}_{\gamma\,64\,Cu}$	s^{-1}	22810	56	0.0
m^{std}	g	0.003260	0.000003	0.0
m^{smp}	g	9.538070	0.000003	0.0
G^{std}_{th}	1	0.9973 [20]	0.0015	
G^{smp}_{th}	1	0.9870 [21]	0.0075	
$G^{std}_{ep,63Cu}$	1	0.9019 [22]	0.0036	
$G^{smp}_{ep,63Cu}$	1	1.0000	0.0000	
f	1	10.9	1.1	
$Q_{0,63Cu}$	1	1.14 [23]	0.23	
r^{std}_{63Cu}	1	1.092	0.021	0.8
r^{smp}_{63Cu}	1	1.092	0.025	1.1
$\varepsilon^{std}_{p,\gamma64Cu}(\varepsilon^{smp}_{p,\gamma64Cu})^{-1}$	1	1.00	0.21	96.3
ρ_{Si}	g cm^{-3}	2.329	0.000	0.0

Table 3. Uncertainty budget of the Cu concentration: k_0 method.

Quantity	Unit	Value	Standard uncertainty	Index
X	[X]	x_i	$u(x_i)$	%
$C^{smp}_{\gamma\,64\,Cu}$	s-1	1.283	0.024	28.0
$C^{smp}_{\gamma\,31\,Si}$	s-1	49540	663	14.0
$S_{31\,Si}$	1	0.7952	0.0000	0.0
$S_{64\,Cu}$	1	0.2792	0.0000	0.0
$k_{0,Au}(^{30}Si,\gamma_{31Si})$	1	1.450×10^{-7} [23]	1.0×10^{-9}	3.8
$k_{0,Au}(^{63}Cu,\gamma_{64Cu})$	1	4.980×10^{-4} [23]	4.5×10^{-6}	6.3
G^{smp}_{th}	1	0.9870 [21]	0.0075	
$G^{smp}_{ep,30Si}$	1	0.9950 [21]	0.0029	
$G^{smp}_{ep,63Cu}$	1	1.0000 [21]	0.0000	
f	1	10.9	1.1	
$Q_{0,30Si}$	1	1.110 [23]	0.067	
$Q_{0,63Cu}$	1	1.14 [23]	0.23	
$r^{smp}_{30\,Si}$	1	1.103	0.012	9.2
$r^{smp}_{63\,Cu}$	1	1.106	0.024	35.8
$\varepsilon^{smp}_{p,\gamma31Si}(\varepsilon^{smp}_{p,\gamma64Cu})^{-1}$	1	1.0691	0.0065	2.9
ρ_{Si}	g cm^{-3}	2.3290	0.0000	0.0
M_{Cu}	g mol^{-1}	63.546	0.003	0.0
N_A	mol^{-1}	6.02×10^{23}	0.000	0.0
Y	[Y]	y	$u_c(y)$	
N_{Cu}	10^{15} cm^{-3}	0.505	0.018	100.0

In the case of the relative method, the main contribution to the 22 % relative standard deviation of the result is the standard to sample ^{64}Cu full-energy γ-peak detection efficiency ratio, $\varepsilon^{std}_{p,\gamma64\,Cu}(\varepsilon^{smp}_{p,\gamma64\,Cu})^{-1}$; the origin of this uncertainty is the position tolerance of 2 mm and the different geometry of the sample and standard. In the case of the k_0 method, the major contributions to the 3.5 % relative standard deviation of the result are the count rates of the ^{64}Cu and ^{31}Si γ-emissions and the total to thermal (n,γ) activation rate ratio of ^{63}Cu, $r^{smp}_{63\,Cu}$; the origins of these uncertainties are the counting statistics, the uncertainty of the $t_{1/2}$ of ^{31}Si and of the Q_0 of ^{63}Cu, respectively.

RESULTS AND DISCUSSION

The Cu concentration was measured six times, after the in-diffusion at 740 °C and after the five out-diffusions at 450 °C. The total irradiation and γ-spectrometry times were 36 h and 224 h, respectively. On average, more than 14 days elapsed between two consecutive irradiations to assure the complete decay of the ^{64}Cu produced in the sample.

Table 4 shows the results obtained with the relative and k_0 standardization method using eqs 1 and 2, respectively; the cy-

cle zero refers to the measurement carried out after in-diffusion. The mass of the sample, m, and the thickness, t_h, of the etched surface-layer are also given.

Table 4. Cu concentration, N_{Cu}, versus the out-diffusion cycle (relative and k_0 method). Cycle zero refers to the measurement carried out after the in-diffusion at 750 °C. The mass of the sample, m, and the thickness, t_h, of the etched surface-layer are also given. The standard uncertainties in parenthesis apply to the last digits.

Cycle	N_{Cu} / 10^{15} cm^{-3}		m / g	t_h / μm
	relative	k_0		
0	1.19(26)	1.303(41)	10.0323	109
1	0.82(18)	0.977(32)	9.9030	29
2	0.57(12)	0.656(25)	9.7580	32
3	0.428(93)	0.502(20)	9.6449	25
4	0.424(93)	0.505(18)	9.5381	24
5	0.419(91)	0.457(14)	9.4090	29

The results are also displayed in Figure 5. Although the values obtained with the relative and k_0 methods are in agreement, they show a systematic offset, which might be due to position and geometry errors affecting the relative method. The Cu concentration value observed in cycle zero, $1.303(41)\times10^{15}$ cm^{-3}, is lower than the 2.2×10^{16} cm^{-3} equilibrium solubility of Cu in Si at 740 °C.[13] Reasons might be an insufficient time to reach the equilibrium concentration and Cu rejoining the metal capping layer during cooling.

The out-diffusion time anticipated by the solution of the diffusion equation to reach a S_{Cu}(450 °C) (actually, 1% higher) at the center of the Si slab initially filled with interstitial Cu at the N_{Cu} value observed in the cycle zero is reported in the second row of Table 1.

The out-diffusion stopped when the Cu concentration decreased to about 0.5×10^{15} cm^{-3}, which is higher than the Cu solubility at 450 °C, 2.4×10^{13} cm^{-3}.[13] We explain the excess by the Cu$_3$Si precipitated into the voids.
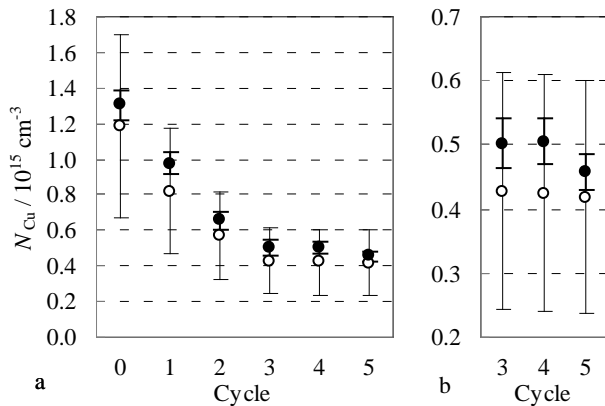

Figure 5. (a) Cu concentration, N_{Cu}, measured with the relative (hollow circles) and k_0 (filled circles) method during the out-diffusion sequence and (b) zoom of the results obtained in the last three cycles. The error bars indicate 95% confidence intervals.

Neutron Damage. Additional lattice defects other than native voids and imperfections are produced during neutron irradiation. Most defects are caused by the direct collision of fast neutrons with Si, resulting in up to 10^3 displacements per event with the interstitial Si moving outside and leaving a vacancy-rich zone. Di-vacancies and clusters are formed by vacancy coalescence and partially recombine with interstitial Si. As a result, the amount of crystal defects per event is smaller than the amount of displacements. In a Si sample irradiated with a fluence of fast neutrons up to 10^{17} cm^{-2}, vacancy-rich zones are heterogeneously distributed. On increasing the fluence above 10^{18} cm^{-2}, the vacancy-rich zones overlap to form homogeneous regions.[24]

The integral flux of fast neutron ($E > 100$ keV) at the irradiation channel used in this study is 6.8×10^{12} cm^{-2} s^{-1}. Figure 5 shows that the interstitial Cu persisted in the lattice until the third cycle, when the total irradiation time was 24 h, corresponding to a fluence of fast neutron of 3.5×10^{18} cm^{-2}. Therefore, during the early out-diffusion cycles, precipitation of Cu in vacancy-rich zones originated by the neutron damage was possible.

Estimate of the Vacancy Concentration. In the case of negligible crystal imperfections, except native voids, the void to sample volume-ratio, e, can be evaluated by

$$e = \frac{\hat{N}_{Cu}}{3 N_A}(V_{m\,Cu3Si} - V_{m\,Si}) \tag{5}$$

where $\hat{N}_{Cu}$ is the Cu concentration in the sample under the assumption that all the void volume is filled with Cu$_3$Si and the interstitial Cu is completely drained, $V_{m\,Si} = 12.058$ cm^3 mol^{-1} is the molar volume of Si, and $V_{m\,Cu3Si} = 1.6\ V_{m\,Si}$ is the molar volume of the η' phase of Cu$_3$Si.[10]

Assuming that the asymptotic value $N_{Cu} = 0.5 \times 10^{15}$ cm^{-3} is an upper limit of $\hat{N}_{Cu}$, the concentration of the vacancies trapped into voids, $N_{vac} = e\ V_{m\,Si}^{-1} N_A$, is expected to be less than 1×10^{14} cm^{-3}. This value is 30 % of the vacancy concentration measured by positron lifetime spectroscopy in the ^{28}Si crystal and used for the N_A determination.[1,4]

CONCLUSIONS

This paper showed that INAA is a chemical analysis method suitable to establish an upper limit to the concentration of the vacancies trapped into voids in single-crystal Si. Experimental evidence was given by measuring the amount of Cu after the in-diffusion at 740 °C, aimed at decorating the voids, and a sequence of out-diffusion at 450 °C, aimed at removing the interstitial Cu. The results are compatible with the eventual observation of stable Cu$_3$Si precipitates.

INAA proved capable to quantify Cu concentrations at 10^{14} cm^{-3} level in a 5 cm^3 volume and 10 g mass Si sample with a relative standard uncertainty from a few percent, k_0 standardization method, to a few tens of percent, relative standardization method.

The preliminary 1×10^{14} cm^{-3} upper limit to the concentration of vacancies trapped into voids of any size is about a third of the value reported for the ^{28}Si Avogadro crystals, which was limited to mono-vacancies, di-vacancies and similar small aggregates. Hence, this measurement can supply a significant upper limit of the total volume of the voids of the spheres used to determine N_A.

REFERENCES

(1) Azuma, Y.; et al. *Metrologia* **2015**, *52*, 360-375.

(2) Zakel, S.; Wundrak, S.; Niemann, H.; Rienitz, O.; Schiel, D. *Metrologia* **2011**, *48***,** S14-S19.

(3) D'Agostino, G.; Di Luzio, M.; Mana, G.; Oddone, M.; Bennett, J. W.; Stopic, A. *Anal. Chem.* **2016**, published online

(4) Andreas, B.; et al. *Metrologia* **2011**, *48*, S1-S13.

(5) Krause-Rehberg, R. *Laboratory Report* University Halle-Wittenberg, Germany **2008**.

(6) Spaepen, F.; Eliat, A. *IEEE T. Instrum. Meas.* **1999**, *48*, 230-232.

(7) Frank, F. C.; Turnbull, D. *Phys. Rev.* **1956**, *104*, 617-618.

(8) Polman, A.; Jacobson, D. C.; Coffa, S; Poate, J. M. *Appl. Phys. Lett.* **1990**, *57*, 1230-1232.

(9) Coffa, S.; Poate, J. M.; Jacobson, D. C. *Phys. Rev. B* **1992**, *45*, 8355-8358.

(10) Wen, C. Y.; Spaepen, F. *Philos. Mag.* **2007**, *87*, 5565-5579.

(11) Landolt-Börnstein *Diffusion in Semiconductors* vol III/33A; Springer-Verlag: Berlin, 1988.

(12) Landolt-Börnstein Impurities and defects in Group IV elements, IV-IV and III-V compounds vol III/41A2; Springer-Verlag: Berlin, 1988.

(13) Weber, E. R. *Appl. Phys A* **1983**, *30***,** 1-22.

(14) Heiser, T.; Mesli, A. *Appl. Phys. A* **1993**, *57***,** 325-328.

(15) Istratov, A. A.; Flink, C.; Hieslmair, H.; Weber, E. R.; Heiser, T. *Phys.Rev.Lett.* **1988**, *81***,** 1243-1246.

(16) Flink, C.; Feick, H.; McHugo, S. A.; Seifert, W.; Hieslmair, H.; Heiser, T.; Istratov, A. A.; Weber, E. R. *Phys. Rev. Lett.* 2000, *85*, 4900-4903.

(17) daRosa, C. P.; Iglesia, E; Maboudian, R. *Electrochim. Acta* **2009**, *54***,** 3270-3277.

(18) GammaVision®, *Version 7.02* by Advanced Measurement Technology, Inc.

(19) BIPM, Evaluation of measurement data – Guide to the expression of uncertainty in measurement.

(20) Martinho, E.; Salgado, J.; Gonçalves, I. F. 2004 *J. Radioanal. and Nucl. Chem.* **2004**, *261*, 637-643.

(21) Chilian, C.; St-Pierre, J.; Kennedy, G. *J. Radioanal. Nucl. Chem.* **2008**, *278*, 745-749.

(22) Martinho, E.; Gonçalves, I. F.; Salgado, J. *Appl. Radiat. Isot.* **2003**, *58*, 371-375.

(23) *Database of recommended k_0-data* released 11.1.2016 by k_0-Nuclear Data Subcommittee of k_0-International Scientific Committee.

(24) Newman, R. C. *Rep. Prog. Phys.* **1982**, *45*, 1163-1210.
.

Table of Contents graphic